# Design of Fusion based Computer Aided Diagnosis Model for Lung Cancer Detection and Classification

**N. Venkatesan**[1] **Dr. S. Pasupathy**[2] **Dr. B. Gobinathan**[3]
[1]Research Scholar, Department of ComputerScience and Engineering, Annamalai University, Chidambaram- 608002, Tamilnadu, India
[2]Associate Professor, Department of ComputerScience and Engineering, Annamalai University, Chidambaram- 608002, Tamilnadu, India
[3]Principal & Professor, Department of ComputerScience and Engineering, Jaya Sakthi Engineering College, Chennai 602024, , Tamilnadu, India
[1]pnvenkatrenu@gmail.com[2]pathyannamalai@gmail.com[3]jeevashanmugi@gmail.com

***Article Info***
***Page Number: 992 – 1005***
***Publication Issue:***
***Vol. 71 No. 3 (2022)***

***Abstract***
Lung cancer remains a serious illness and results in high mortality rate over the globe. Earlier identification of lung cancer based on computed tomography (CT) images helps to diagnose the disease and increase the survival rate. Computer aided diagnosis (CAD) models can be designed for lung cancer diagnosis using different processes such as preprocessing, segmentation, feature extraction, and classification. With this motivation, this study designs a fusion based CAD model for lung cancer detection and classification (FCAD-LCDC). The goal of the FCAD-LCDC technique is for detecting and classifying different types of lung cancer using CT images. The FCAD-LCDC technique involves Gaussian filtering (GF) as a preprocessing approachfor removing the noise that exists in the CT images. Besides, a fusion of Inceptionv3 based deep features and histogram of gradients (HOG) based handcrafted features take place for feature extraction. Moreover, extreme gradient boosting (XGBoost) classifier is used to allot proper class labels to the applied CT images. In order to showcase the better outcome of the FCAD-LCDC technique, a series of simulations were carried out on the benchmark dataset and the results portrayed the supremacy of the FCAD-LCDC technique over the other CAD models interms of different measures.

**Keywords:** Computer aided diagnosis, Lung cancer, Image processing, Deep learning, Fusion model, XGBoost classifier

***Article History***
***Article Received:*** *12 January 2022*
***Revised:*** *25 February 2022*
***Accepted:*** *20 April 2022*
***Publication:*** *09 June 2022*

## 1. Introduction

Lung cancer is the primary cause of cancer death in males and females. It is evaluated that 1.2 million people are detected by these diseases yearly (12.3% of the overall amount of cancer detected), and around 1.1 million people are passing away from these diseases every year (17.8% of the overall cancer deaths) [1]. The survival rates are high when the cancer is detected in the early stage. About 80% of persons were detected properly in the middle or final stages of cancer [2]. Computer aided diagnoses (CAD) system is highly useful for radiologists in diagnosing and detecting abnormalities faster and earlier. The CAD is the 2nd perspective for radiologists beforehand proposing biopsy tests [3]. In current study, it is noted that principles of neural networks are employed broadly for the diagnoses of lung cancer in medicinal images [4]. For classifications of lung cancer, some approaches that depend on NN were stated in this survey.

Asuntha and Srinivasan [5] detects the tumorous lung nodule from the provided input lung images and for classifying the severity and lung cancer its. In order to identify the position of tumorous lung nodule, this study employs new DL approaches. This study employs optimal FE methods like HoG, Zernike Moment, SIFT, LBP and wavelet transform based features. Afterward extracting geometric, texture, intensity, and volumetric features, FPSO method is used to select optimal features. Lastly, this feature is categorized with DL methods. In Saba et al. [6], DL was presented as potential tool for classifying malignant nodules. The goal is to retrospectively authenticate LCP-CNN model that is trained on US screening data, on self-governing datasets of indeterminate nodule in a European multicenter trial, for excluding benign nodule maintains a higher lung cancer sensitivity.InLakshmanaprabu et al. [7], the CT scan of lung image has been examined using ODNN and LDA models. The deep features extracted from a CT lung image also dimension of features are decreased by the LDR for classifying lung nodules as benign/malignant. The ODNN is used for CT images, also enhanced by an MGSA method to detect the lung cancer classifications.

Wang et al. [8] presented weakly supervised approaches for effective and fast classifications on the entire slide lung cancer images. This technique initially utilize patch based FCN for retrieving discriminate block and provide descriptive deep feature using higher efficacy. Next, feature aggregation and distinct context aware block selection approaches are examined for generating global holistic WSI descriptors i.e., eventually fed to RF classifiers for the image level predictions. Weng et al. [9] demonstrate the possibility of using a DL method for manually distinguish cancerous and normal lung tissue images obtained from CARS. They leverage the feature learned by pre-trained DNN and maintain the models by means of CARS image as the input.

InAusawalaithong et al. [10], the 121 layer CNN, called DenseNet-121 proposed by G. Huang et al., and TL system is examined as a means of categorizing lung cancer via chest x-ray image. The method has been trained on lung nodules beforehand training on lung cancer datasets for alleviating the problems of employing smaller datasets.Mahesh et al. [11] developed a CAD scheme for finding the lung cancer through the lung CT image also categorize the nodules as Malignant/Benign. In order to classify cancer cells, SVM classifiers are employed. Now, image processing methods are employed for enhancing, de-noise, segmenting, and edge detecting of images are employed for extracting the shape, area, and perimeter of the nodules.

InShariaty and Mousavi [12], the applications of CAD system for the diagnoses of lung cancer was explored – involving segmentation, data analysis, and pre-processing approaches. The major aim is to examine the most recent technologies for the growth of computer diagnostic tools, for assisting the analysis, acquisition, and processing of medicinal imaging data. Chellan and Chellappan [13] focuses on discovering the tumorous area and categorize the lung cancer CT image. The presented method plays an important part in identifying the type of tumorous area in the lung CT image and help radiologist for enhancing the diagnoses in healthcare of a patient. Also, it is lesser time consuming procedure in categorizing the lung CT image. BoVW method is a new classification method i.e., employed on lung CT images for classifying the clusters of malignant/benign lung cancer in distinct stages.

This study designs a fusion based CAD model for lung cancer detection and classification (FCAD-LCDC) for detecting and classifying different types of lung cancer using CT images. The FCAD-LCDC technique involves Gaussian filtering (GF) as a preprocessing approach for removing the noise that exists in the CT images. Besides, a fusion of Inceptionv3 based deep features and histogram of gradients (HOG) based handcrafted features take place for feature extraction. Moreover, extreme gradient boosting (XGBoost) classifier is used to allot proper class labels to the applied CT images. In order to showcase the better outcome of the FCAD-LCDC technique, a series of simulations were carried out on the benchmark dataset

## 2. The Proposed FCAD-LCDC technique

In this study, a new FCAD-LCDC technique is designed for detecting and classifying different types of lung cancer using CT images. The FCAD-LCDC technique involves GF based preprocessing, fusion of Inceptionv3 based deep features, and HOG based handcrafted features for feature extraction. Furthermore, the XGBoost classifier is used to allot proper class labels to the applied CT images. Fig. 1 demonstrates the overall working process of FCAD-LCDC model. The working detail of these modules is givenin the following.

### 2.1. Preprocessing using GF Technique

The implementation of 2D GF was utilized widely to smooth as well as eradicate noise. It requires enormous process resources and the performance in executing is a stimulating analysis. The convolutional functions were determined as Gaussian operator and offer of Gaussian smoothing has been able by convolutional. The Gaussian operator from 1-D has been given as:

$$G_{1D}(x) = \frac{1}{\sqrt{2\pi}\sigma} e^{-\left(\frac{x^2}{2\sigma^2}\right)}. \tag{1}$$

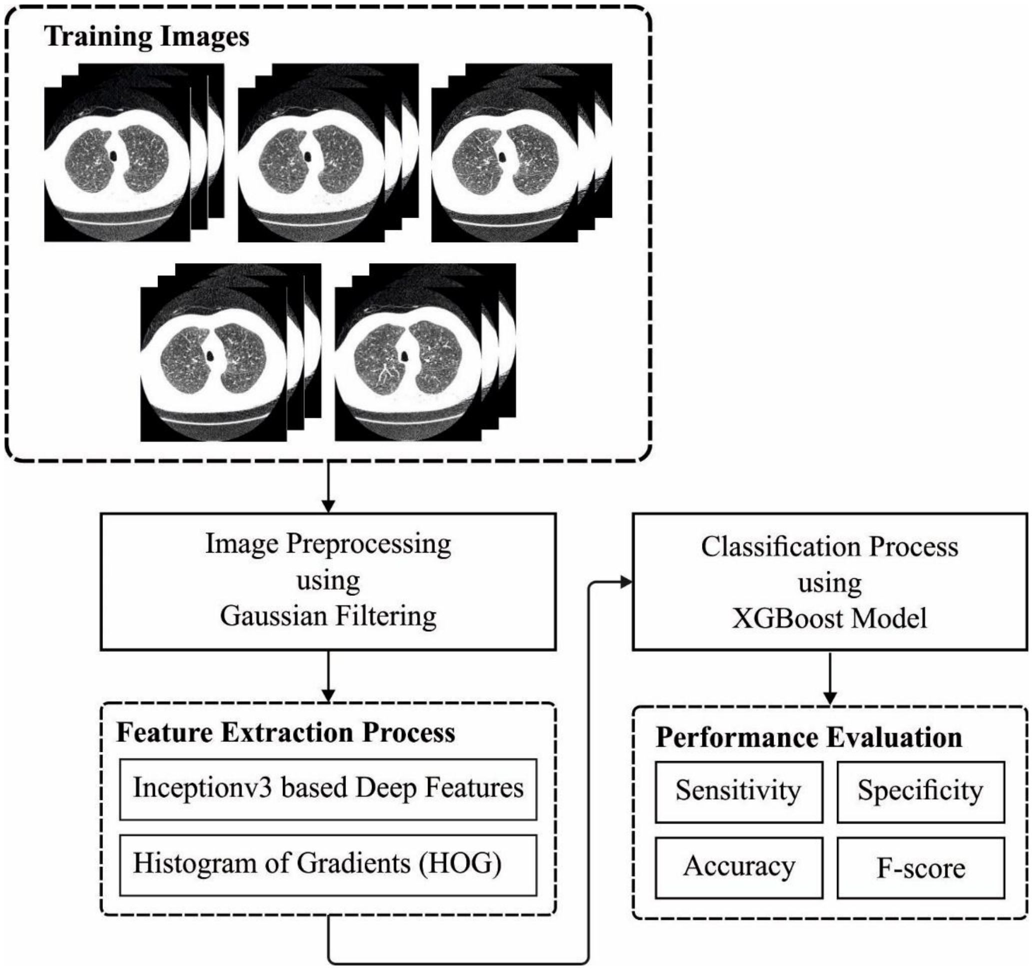


**Fig. 1. Overall process of FCAD-LCDC model**

Optimum smooth filtering to images endures localization from the spatial and frequency domain, in which the uncertainty relation has been fulfilled as:

$$\Delta x \Delta \omega \geq \frac{1}{2}. \tag{2}$$

The Gaussian operator from 2D was defined as:

$$G_{2D}(x,y) = \frac{1}{2\pi\sigma^2} e^{-\left(\frac{x^2+y^2}{2\sigma^2}\right)}, \tag{3}$$

where σ (Sigma) refers the SD of Gaussian function [14]. If the maximal values, the image smooth is higher. $(x, y)$ stands for the Cartesian coordinates of an image which illustrates the dimensional of window.

### 2.2. Fusion based Feature Extraction

The preprocessed image is fed into the fusion model where the handcrafted as well as deep features are extracted.

#### 2.2.1. Inception V3 Model

The main objective of GoogLeNet network is an Inception network framework, the GoogLeNet technique is termed as Inception networks [15]. It involves of maximal GoogLeNet version which is categorized as to distinct versions of Inception v1, Inception v2, Inception v3, Inception v4, and Inception-ResNet. Therefore, an Inception usually involves 3 distinct sizes of convolutional as well as maximal pooling. The outcome of network from preceding layer was determined as channel is gathered once afterward implementation convolutional task, and non-linear fusion is implemented. Likewise, the expression function of this network and applicable to different scales that are improving, and eliminating the over-fitting issue. Fig. 2 shows the Inception V3 framework.

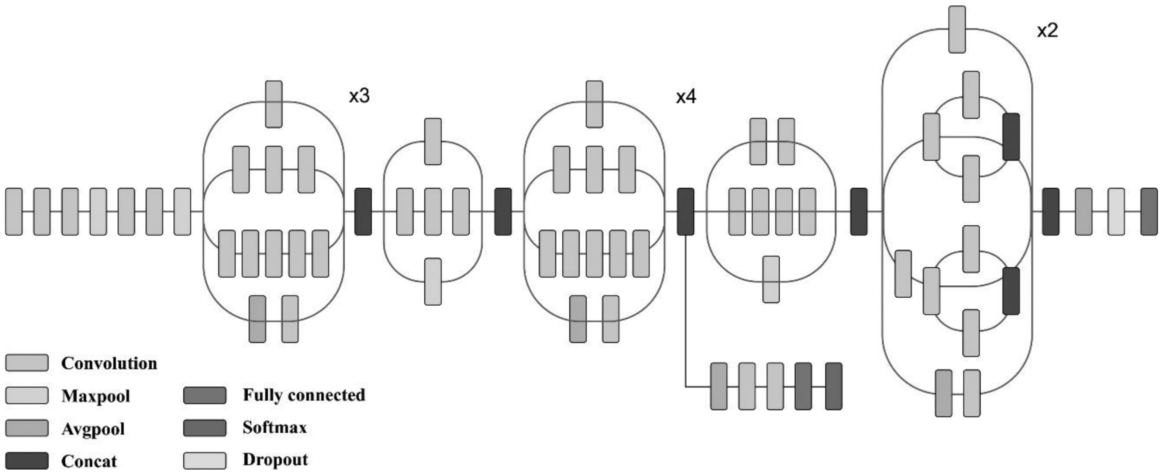


**Fig. 2. Structure of Inception V3 Model**

An inception v3 mentions that network framework utilized by Keras which has pre-training from Image Net. If related to Inception v1 and v2, Inception v3 network framework utilizes the convolutional kernel split technique to divide enormous volume integrals as to minimal convolutional. For sample, a 3*3 convolutional is separated as to 3*1 and 1*3 convolutional. With utilizing this splitting technique, the amount of attributes are restricted, therefore, the network training speed is triggered at the time of removing spatial feature from effectual method. Likewise, an inception v3 optimizations the Inception network framework with use of 3 distinct sized grids such as 35*35, 17*17, and 8*8.

### 2.2.2. HOG Features

An essential feature in HOG feature is capable of holding the local form of object and account the invariance of object conversion and illumination status as edge and data concerning gradient is evaluated by utilizing several coordinate-HOG feature vectors. Primarily, the gradient operator N is executed for defined the gradient measure. The gradient point of mammogram image has been projected as G and image frame is demonstrated as I. The general equation utilized from computing gradient point is pointed in Eq. (4):

$$G_x = N * I(x,y) and\ G_x = N^T * I(x,y) \quad (4)$$

An image detect window endures characterized as varied spatial regions which are called cells. So, the magnitude gradients of pixels were executed with edge orientation [16]. Thus the outcome, the magnitude of gradient (x, y) has been applied in Eq. (5).

$$G_x(x,y) = \sqrt{G_x(x,y)^2} + \sqrt{G_y(x,y)^2} \quad (5)$$

The edge orientation of point (x, y) has been offered in Eq. (6):

$$\theta(x, y) = \tan^{-1}\frac{G_y(x, y)}{G_x(x, y)} \quad (6)$$

where $G_x$ signifies the horizontal way of gradients and $G_y$ refers the vertical way of gradients. In the event, an improvement for illuminating and noise, a normalized task has been managed once implementation the histogram measure. The purpose of normalized has been utilized from contrast as well as local histograms are estimated. In several coordinates HOG, 4 varied manners of normalized are implemented such as L2-norm, L2-Hys, L1-Sqrt, and L1-norm. If related to this normalized, L2-norm offers the optimum functions in cancer forecast. The segment normalized in HOG is written in Eq. (7).

$$\mathrm{L2-norm:}\ \mathrm{f} = \frac{\mathrm{h}}{\sqrt{||h||_2^2 + \mathrm{e}^2}} \quad (7)$$

where $e$ refers the small positive value utilized from regularization, $f$ defines the feature vector, $h$ illustrates the non-normalization vector, and $||h||_2^2$ represents the two-norm of HOG normalization.

### 2.2.3. Fusion process

The data fusion was utilized from varied ML and computer vision sectors. The feature fusion was an important function which combines maximal feature vectors. The presented technique is dependent upon features fusion with entropy. Also, the feature that is attained has integrated as to single vector. There are two vectors that are calculated as:

$$f_{Inception\ \_v3\times m} = \{Inception\_v3_{1\times 1}, Inception\_v3_{1\times 2}, Inception\_v3_{1\times 3}, \ldots, Inception\_v3_{1\times n}\} \quad (8)$$

$$f_{HOG1\times p} = \{HOG_{1\times 1}, HOG_{1\times 2}, HOG_{1\times 3}, \ldots, HOG_{1\times n}\} \quad (9)$$

Afterward, the feature extraction has integrated as single vector.

$$Fused\ (feature\ vector)_{1\times q} = \sum_{i=1}^{2}\{fInceptionV3_{1\times m}, fHOG_{1\times p}\} \quad (10)$$

where $f$ refers the fused vector. The entropy has been executed on feature vectors to only elected features that are dependent upon values.

$$B_{He} = -NHe_b\sum_{i=1}^{n} p(f_i) \quad (11)$$

$$F_{select} = B_{He}(\max(f_i, 1186)) \quad (12)$$

In Eqs. (11) and (12), $p$ refers the features probabilities and $He$ signifies the entropy.

## 2.3. Image Classification using XGBoost

The fused feature vectors are passed into the XGBoost model to perform classification process. Chen and Guestrin proposed an XGBoost, which is a strong approach for the classification and regression models. This can be used as a set of winning programs from Kaggle ML competition. XGBoost is depend on gradient boosting architecture, continuously adds a novel DT to fit a value using multiple residual iterations also improves the performance and efficiency of learners. Different from gradient boosting, XGBoost uses a

Taylor expansion for approximating the loss function, as well as the method has an optimal trade-off variance and bias, commonly employing less DT for obtaining a high precision Detail of XGBoost is listed as follows. Assume a provided sample sets have $n$ sample and $m$ feature; it is formulated by $= \{(x_i, y_i)\}(|D| = n, x_i \in R^m, y_i \in R)$, whereas $x$ denotes the eigenvalue, and $y$ indicates the true values. The approach adds the result of $K$ trees as the last prediction values that can be formulated by

$$y_j = \sum_{k=1}^{K} f_k\,(x_i), f_k \in F \tag{13}$$

$F$ represent the group of DTs, by:

$$F = \{f(x) = w_{q(x)}\}(q: R^m \to T, w \in R^T)$$

Whereas $f(x)$ is most of trees, and $w_{q(x)}$ represents the weight of leaf node. $T$ indicate the amount of leaves node, and $q$ represent the structures of every tree, that map the samples to the equivalent leaf nodes [17]. Hence, the prediction values of XGBoost are the amount of the values of the leaf node of all trees. The aim is for learning this $k$ tree, hence minimalize the succeeding objective function:

$$L^{(t)} = \sum_{i=1}^{n} l\,(y_i, \widehat{y_i}) + \sum_{k=1}^{K} \Omega\,(f_k) \tag{14}$$

$l$ denotes the loss of the differences among the evaluated values $y_i$ and the true valued $y_i$,· general loss function includes the exponential, logarithmic, and square loss functions. $\Omega$ standardization is employed for setting the penalty of DT, that could avoid overfitting. $\Omega$ is given below:

$$\Omega(f) = \gamma T + \frac{1}{2}\lambda\|\omega\|^2 \tag{15}$$

In standard terms, $\gamma$ denotes a hyperparameter which controls the difficulty of the method, and $T$ indicate the amount of leaves node. $\lambda$ denotes the penalty coefficients for the leaf weight $\omega$, that is generally constant. $\gamma \& \lambda$ determines the difficulty of the method and are generally provided empirically at the time of training, a novel trees are included to fit the residual of the prior rounds.

## 3. Results and Discussion

The experimental validation of the FCAD-LCDC technique takes place on benchmark dataset [18]. The dataset includes three class labels namely benign, malignant, and normal. The number of images under these classes is 32, 33, and 35. Fig. 3 showcases a few of the sample test images.

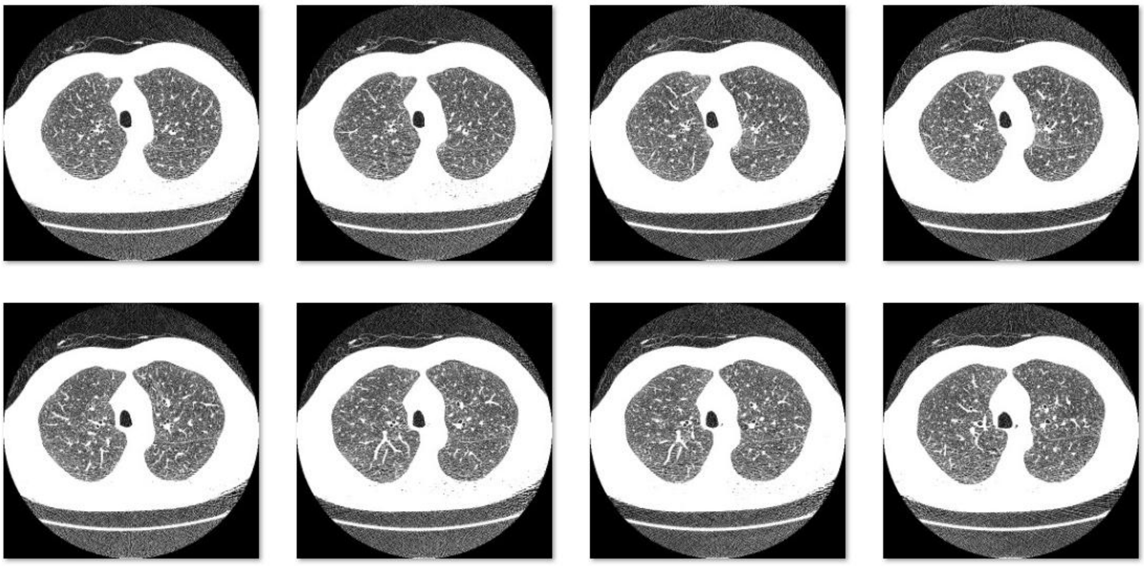

**Fig. 3. Sample Images**

The confusion matrices produced by the FCAD-LCDC technique on the execution of three distinct runs are given in Fig. 4. The results have shown that the FCAD-LCDC technique has resulted in maximum classification outcomes. For instance, with run-1, the FCAD-LCDC technique has categorized the 34 images into Normal, 32 images into Malignant, and 32 images into Benign. Afterward, with run-2, the FCAD-LCDC approach has categorized the 34 images into Normal, 32 images into Malignant, and 31 images into Benign. Simultaneously, with run-3, the FCAD-LCDC algorithm has categorized the 34 images into Normal, 31 images into Malignant, and 31 images into Benign.

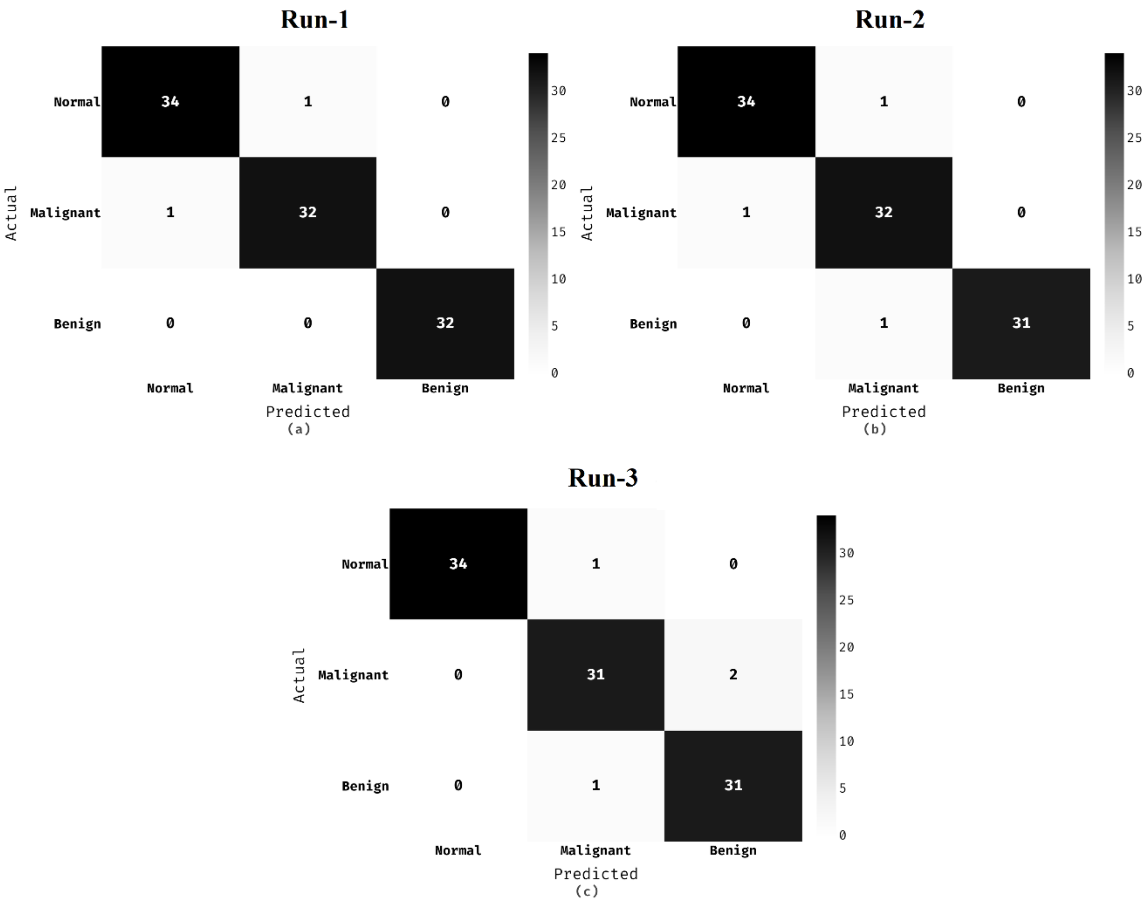


**Fig. 4. Confusion matrix of FCAD-LCDC model**

An extensive overview of the classification results accomplished by the FCAD-LCDC technique is given in Table 1. The results demonstrated that the FCAD-LCDC technique has resulted in maximum classification performance. For instance, under run-1, the FCAD-LCDC technique has obtained an average sensitivity of 0.980, specificity of 0.990, accuracy of 0.980, and F-score of 0.971. In addition, under run-2, the FCAD-LCDC manner has attained an average sensitivity of 0.970, specificity of 0.985, accuracy of 0.980, and F-score of 0.970. Moreover, under run-3, the FCAD-LCDC methodology has reached an average sensitivity of 0.960, specificity of 0.980, accuracy of 0.973, and F-score of 0.960.

**Table 1** Result analysis of FCAD-LCDC model with different measures

| **Metrics** | **Sensitivity** | **Specificity** | **Accuracy** | **F-Score** |
|---|---|---|---|---|
| **Run-1** | | | | |
| Normal | 0.971 | 0.985 | 0.980 | 0.971 |
| Malignant | 0.970 | 0.985 | 0.980 | 0.970 |
| Benign | 1.000 | 1.000 | 1.000 | 1.000 |
| **Average** | **0.980** | **0.990** | **0.987** | **0.980** |
| **Run-2** | | | | |
| Normal | 0.971 | 0.985 | 0.980 | 0.971 |

| | | | | |
|---|---|---|---|---|
| Malignant | 0.970 | 0.970 | 0.970 | 0.955 |
| Benign | 0.969 | 1.000 | 0.990 | 0.984 |
| **Average** | **0.970** | **0.985** | **0.980** | **0.970** |
| **Run-3** | | | | |
| Normal | 0.971 | 1.000 | 0.990 | 0.986 |
| Malignant | 0.939 | 0.970 | 0.960 | 0.939 |
| Benign | 0.969 | 0.971 | 0.970 | 0.954 |
| **Average** | **0.960** | **0.980** | **0.973** | **0.960** |

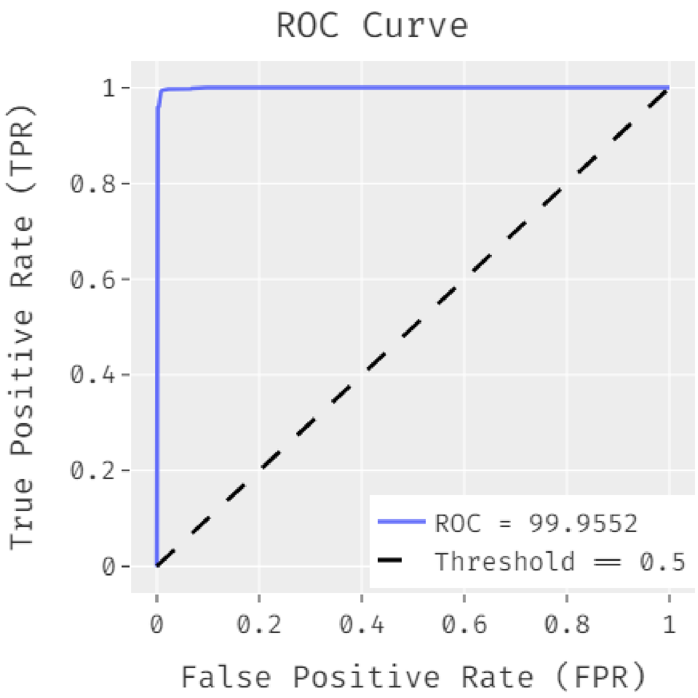


**Fig. 5. ROC analysis of FCAD-LCDC model**

The ROC analysis of the FCAD-LCDC technique on the applied dataset is offered in Fig. 5. The results depicted that the FCAD-LCDC technique has resulted in a higher ROC of 99.9552.

In order to ensure the betterment of the FCAD-LCDC technique, a detailed comparison study is made in Table 2. Fig. 6 investigates the results analysis of the FCAD-LCDC technique with existing techniques reported that the FCAD-LCDC technique has accomplished a higher sensitivity of 0.98 whereas the CN-SVM, MLP-CM, RBF-CM, LR-CM, ANN-CM, and KNN-CM techniques have obtained a reduced sensitivity of 0.95, 0.82, 0.84, 0.77, 0.86, and 0.91 respectively.

**Table 2 Comparative analysis of FCAD-LCDC model with existing techniques**

| **Methods** | **Sensitivity** | **Specificity** | **Accuracy** |
|---|---|---|---|
| FCAD-LCDC | 0.98 | 0.99 | 0.99 |
| CN-SVM | 0.95 | 0.93 | 0.96 |

| | | | |
|---|---|---|---|
| MLP-CM | 0.82 | 0.77 | 0.72 |
| RBF-CM | 0.84 | 0.86 | 0.54 |
| LR-CM | 0.77 | 0.89 | 0.36 |
| ANN-CM | 0.86 | 0.87 | 0.79 |
| KNN-CM | 0.91 | 0.90 | 0.83 |

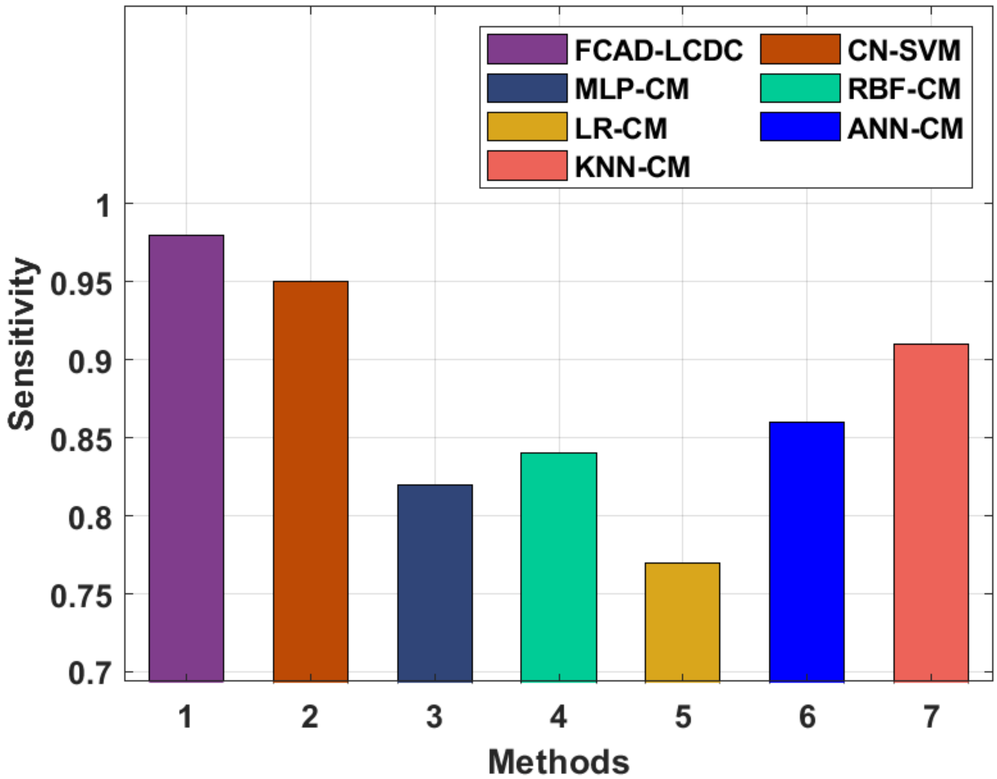


**Fig. 6. Sensitivity analysis of FCAD-LCDC model with recent approaches**

Fig. 7 examines the outcomes analysis of the FCAD-LCDC manner with recent approaches demonstrated that the FCAD-LCDC algorithm has accomplished an increased specificity of 0.99 whereas the CN-SVM, MLP-CM, RBF-CM, LR-CM, ANN-CM, and KNN-CM methods have reached a minimal specificity of 0.93, 0.77, 0.86, 0.89, 0.87, and 0.90 correspondingly.

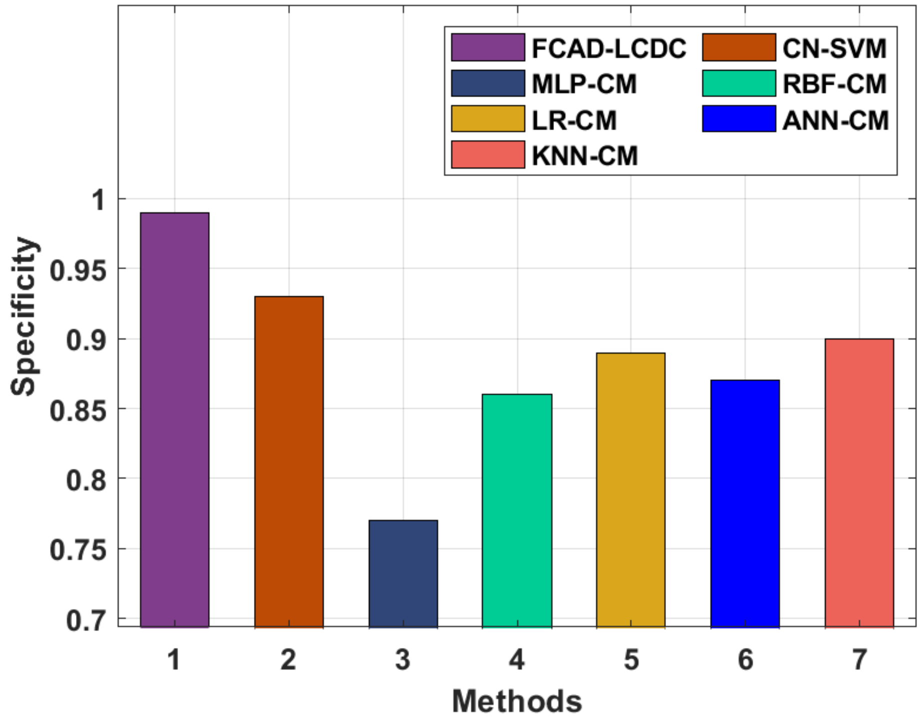


**Fig. 7. Specificity analysis of FCAD-LCDC model with recent approaches**

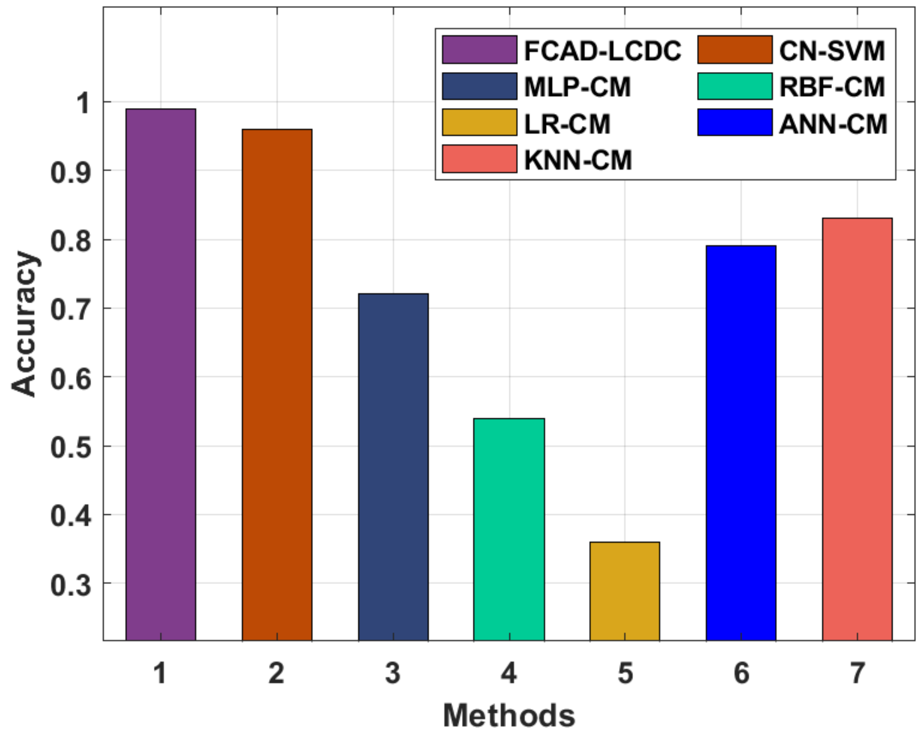


**Fig. 8. Accuracy analysis of FCAD-LCDC model with recent approaches**

Fig. 8 explores the outcomes analysis of the FCAD-LCDC method with state-of-art methods showcased that the FCAD-LCDC manner has accomplished a superior accuracy of 0.98 whereas the CN-SVM, MLP-CM, RBF-CM, LR-CM, ANN-CM, and KNN-CM methodologies have gained a diminished accuracy of 0.96, 0.72, 0.54, 0.36, 0.79, and 0.83 correspondingly.

## 4. Conclusion

In this study, a new FCAD-LCDC technique is designed for detecting and classifying different types of lung cancer using CT images. The FCAD-LCDC technique involves GF based preprocessing, fusion of Inceptionv3 based deep features, and HOG based handcrafted features for feature extraction. Furthermore, the XGBoost classifier is used to allot proper class labels to the applied CT images. In order to showcase the better outcome of the FCAD-LCDC technique, a series of simulations were carried out on the benchmark dataset and the results are investigated under diverse aspects. The results portrayed the supremacy of the FCAD-LCDC technique over the other CAD models interms of different measures. Therefore, the FCAD-LCDC technique can be utilized as an effective tool to diagnose CAD techniques. In future, the diagnostic outcome of the FCAD-LCDC technique can be raised by the design of segmentation approaches.

## References

[1] Kuruvilla, J. and Gunavathi, K., 2014. Lung cancer classification using neural networks for CT images. *Computer methods and programs in biomedicine*, *113*(1), pp.202-209.

[2] A. Motohiro, H. Ueda, H. Komatsu, N. Yanai, T. Mori, Prognosis of non-surgically treated, clinical stage I lung cancer patients in Japan, Lung Cancer 36 (2002) 65–69.

[3] A.A. Abdulla, S.M. Shaharum, Lung cancer cell classification method using artificial neural network, Information Engineering Letters 2 (March) (2012) 50–58.

[4] G. Coppini, S. Diciotti, M. Falchini, N. Villari, G. Valli, Neural networks for computer aided diagnosis: detection of lung nodules in chest radiograms, IEEE Transactions on Information Technology in Biomedicine 4 (2003) 344–357.

[5] Asuntha, A. and Srinivasan, A., 2020. Deep learning for lung Cancer detection and classification. Multimedia Tools and Applications, 79(11), pp.7731-7762.

[6] Saba, T., Kashif, M., Alaskar, H. and Afzal, E., 2021. 6 Lung Cancer Detection and Diagnosis with Deep Learning Models Evaluation. *Artificial Intelligence and Internet of Things: Applications in Smart Healthcare*, p.167.

[7] Lakshmanaprabu, S.K., Mohanty, S.N., Shankar, K., Arunkumar, N. and Ramirez, G., 2019. Optimal deep learning model for classification of lung cancer on CT images. Future Generation Computer Systems, 92, pp.374-382.

[8] Wang, X., Chen, H., Gan, C., Lin, H., Dou, Q., Tsougenis, E., Huang, Q., Cai, M. and Heng, P.A., 2019. Weakly supervised deep learning for whole slide lung cancer image analysis. IEEE transactions on cybernetics, 50(9), pp.3950-3962.

[9] Weng, S., Xu, X., Li, J. and Wong, S.T., 2017. Combining deep learning and coherent anti-Stokes Raman scattering imaging for automated differential diagnosis of lung cancer. Journal of biomedical optics, 22(10), p.106017.

[10] Ausawalaithong, W., Thirach, A., Marukatat, S. and Wilaiprasitporn, T., 2018, November. Automatic lung cancer prediction from chest X-ray images using the deep learning approach. In 2018 11th Biomedical Engineering International Conference (BMEICON) (pp. 1-5). IEEE.

[11] Mahesh, S., Rakesh, S. and Patil, V.C., 2018, April. Computer aided detection system for lung cancer using computer tomography scans. In AIP Conference Proceedings (Vol. 1952, No. 1, p. 020101). AIP Publishing LLC.

[12] Shariaty, F. and Mousavi, M., 2019. Application of CAD systems for the automatic detection of lung nodules. Informatics in Medicine Unlocked, 15, p.100173.

[13] Chellan, T.D. and Chellappan, A.K., 2018. Novel computer-aided diagnosis of lung cancer using bag of visual words to achieve high accuracy rates. The Journal of Engineering, 2018(12), pp.1941-1946.

[14] Särkkä, S. and Sarmavuori, J., 2013. Gaussian filtering and smoothing for continuous-discrete dynamic systems. *Signal Processing*, *93*(2), pp.500-510.

[15] Wang, C., Chen, D., Hao, L., Liu, X., Zeng, Y., Chen, J. and Zhang, G., 2019. Pulmonary image classification based on inception-v3 transfer learning model. *IEEE Access*, *7*, pp.146533-146541.

[16] Satpathy, A., Jiang, X. and Eng, H.L., 2013. Human detection by quadratic classification on subspace of extended histogram of gradients. *IEEE Transactions on Image Processing*, *23*(1), pp.287-297.

[17] Jiao, W., Hao, X. and Qin, C., 2021. The Image Classification Method with CNN-XGBoost Model Based on Adaptive Particle Swarm Optimization. *Information*, *12*(4), p.156.

[18] http://www.via.cornell.edu/lungdb.html